

Compression of 1.8 μm laser pulses to sub two optical cycles with bulk material

Bruno E. Schmidt,^{1,2,a)} Pierre Béjot,³ Mathieu Giguère,¹ Andrew D. Shiner,² Carlos Trallero-Herrero,² Éric Bisson,¹ Jérôme Kasparian,⁴ Jean-Pierre Wolf,⁴ David M. Villeneuve,² Jean-Claude Kieffer,¹ Paul B. Corkum,² and François Légaré^{1,a)}

¹Centre Énergie Matériaux et Télécommunications, Institut National de la Recherche Scientifique, 1650 Boulevard Lionel-Boulet, Varennes, Quebec J3X1S2, Canada

²Joint Laboratory for Atto-Second Science, University of Ottawa/NRC, 100 Sussex Drive, Ottawa, Ontario K1A 0R6, Canada

³Laboratoire Interdisciplinaire CARNOT de Bourgogne, UMR 5209 CNRS, Université de Bourgogne, BP 47870, 21078 Dijon Cedex, France

⁴GAP-Biophotonics, Université de Genève, 20 rue de l'École de Médecine, 1211 Geneva 4, Switzerland

(Received 20 January 2010; accepted 17 February 2010; published online 25 March 2010)

We demonstrate a simple scheme to generate 0.4 mJ 11.5 fs laser pulses at 1.8 μm . Optical parametrically amplified pulses are spectrally broadened by nonlinear propagation in an argon-filled hollow-core fiber and subsequently compressed to 1.9 optical cycles by linear propagation through bulk material in the anomalous dispersion regime. This pulse compression scheme is confirmed through numerical simulations. © 2010 American Institute of Physics. [doi:10.1063/1.3359458]

In the past decade, attosecond technology based on high harmonic generation has been developed permitting ultrafast measurements with ~ 100 as temporal resolution.¹⁻³ Further reduction in the duration of isolated attosecond pulses and higher photon energies requires intense longer-wavelength carrier envelope phase (CEP) stable few-cycle pulses. Those requirements can be fulfilled using the Idler of a white light seeded optical parametric amplifier (OPA)⁴ with an appropriate pulse compression scheme. In this letter, we demonstrate a robust approach for pulse compression at 1.8 μm to below two optical cycle duration.

Different approaches to generate intense IR few-cycle laser pulses have been demonstrated as follows: (1) 0.74 mJ 15.6 fs at 2.1 μm using an optical parametric chirped-pulse amplifier (OPCPA),⁵ (2) pulse self-compression by filamentation; 0.27 mJ 17.9 fs at 2.1 μm ⁶ and 1.5 mJ 19.8 fs at 1.5 μm ,⁷ (3) 1.2 mJ 17 fs at 1.5 μm utilizing difference frequency generation of few-optical-cycle 800 nm laser pulses followed by type II parametric amplification,⁸ and (4) 0.4 mJ 13.1 fs at 1.4 μm using spectral broadening in a hollow-core fiber (HCF) and dispersion compensation with chirped mirrors.⁹

In this letter, we demonstrate the generation of 0.4 mJ 11.5 fs laser pulses at 1.8 μm . Similar to our recent work using the OPA Signal wavelength,⁹ we spectrally broaden the Idler via nonlinear propagation in a HCF. Instead of chirped mirrors or adaptive devices for dispersion compensation, we show that laser pulses can be efficiently compressed utilizing solely the properties of fused silica (FS) in the anomalous dispersion regime below the third order dispersion (TOD) limit of bulk material. Although compression with glass in the anomalous dispersion regime was applied to mid-IR wavelengths ($\sim 6 \mu\text{m}$),¹⁰ the authors discussed the limitation of bulk material compression to be applicable to multi-cycle pulses only.

The present approach distinguishes itself from previous setups in the reduced complexity, as shown in the sketch of the experimental layout in Fig. 1(a). The IR laser pulses are generated with a superfluorescence-seeded three stage OPA (HE-TOPAS, Light conversion) pumped by 7 mJ, 45 fs Ti:Sa pulses. A conversion efficiency of 35% (Signal+Idler) with 3% intensity fluctuation is typically achieved at the OPA output. At 1.83 μm , the spectral full width at half maximum (FWHM) is 67 nm corresponding to a TL of 73 fs. This OPA spectrum, shown as shaded gray in Fig. 1(b), is measured with an Ocean Optics NIR 256 spectrometer corrected for spectral sensitivity. The IR laser beam is coupled into a 1 m long HCF (400 μm in diameter, argon pressure of 140 ± 10 kPa, 1 mm CaF_2 windows) using a $f=1$ m plano-convex CaF_2 lens. At the output, the laser beam is collimated

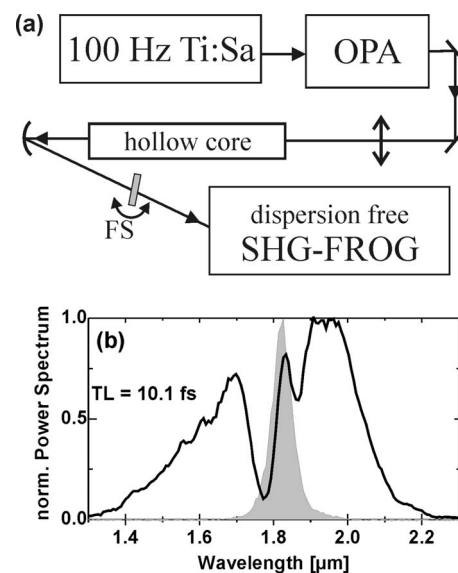


FIG. 1. (a) Experimental layout comprising a CPA pumped high energy OPA whose spectrum is broadened via propagation in a HCF. (b) Experimental spectra of the OPA Idler before (shaded gray) and after broadening (solid black). An asymmetric broadening towards the blue spectral side is visible.

^{a)}Authors to whom correspondence should be addressed. Electronic addresses: schmidt@emt.inrs.ca and legare@emt.inrs.ca.

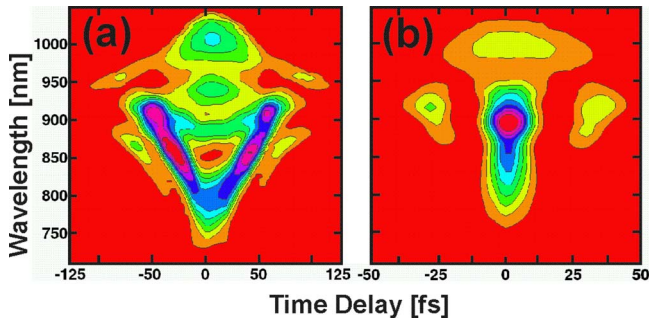


FIG. 2. (Color online) Experimental SHG-FROG traces for the uncompressed pulse after propagation in the HCF (a) corresponds to a pulse duration of 68 fs. Propagation through 3 mm of FS leads to a compressed 11.5 fs pulse depicted in (b) on a different time scale.

with an $R=2$ m concave silver mirror. As shown by the solid line of Fig. 1(b), with 0.89 mJ at the input of the HCF, significant spectral broadening is observed corresponding to a TL of 10.1 fs. This spectrum clearly shows an asymmetry with wider extension towards shorter wavelengths.

Complete pulse characterization is carried out with a home built SHG-FROG (second harmonic generation frequency resolved optical grating).¹¹ Beam splitting is attained by geometrical beam separation to achieve ultrabroadband and dispersion free operation.¹² A high degree of phase matching and negligible geometrical temporal smear¹³ is obtained by achromatically focusing both optical arms with a 500 mm focal length convex silver mirror into a Type I BBO crystal ($\theta=21^\circ$) of 10 μm thickness. The SHG-FROG spectrograms are measured with a USB2000 spectrometer from Ocean Optics and corrected for spectral sensitivity. In addition, spectral distortion of the ultrabroadband SHG is accounted for by applying a cubic correction function to the measured SHG-FROG spectrogram.¹³

After spectral broadening in the HCF, the pulse must be temporally compressed. At 800 nm, this is commonly carried out with chirped mirrors which are not available at 1.8 μm . Fortunately, the unique characteristics of the 1.8 μm source mean that the negative group delay dispersion (GDD) of FS is able to compensate for the spectral phase introduced by self-phase modulation (SPM) in argon. Because the zero dispersion of FS lies at ~ 1.3 μm , it exhibits negative GDD throughout the entire spectral range of interest. Once the appropriate FS thickness is found, a small angular tilt of the glass is sufficient to obtain the shortest pulse duration. In this manner a compression factor of 6.5 is achieved compared to the OPA output pulses.

The pulse duration immediately after the evacuated fiber was measured to be 75 fs [Fig. 3(c), gray line] in agreement with the TL (73 fs) of the OPA spectra presented in Fig. 1(b) as shaded gray. Inserting argon leads to significant broadening and the corresponding SHG-FROG traces of the uncompressed and fully compressed pulses are shown in Fig. 2. Surprisingly, linear propagation through a simple piece of FS is sufficient to achieve excellent compression. Figure 3 presents the reconstructed electric field in the spectral (a, b) and the temporal domains (c). The direction of the time axis was determined by comparing the spectral phase with and without the 3 mm FS. The asymmetric shape of the reconstructed power spectrum [solid black line in Fig. 3(a)] is in reasonable agreement with the measured one given by the black squares. The spectral phase for the compressed pulse [black

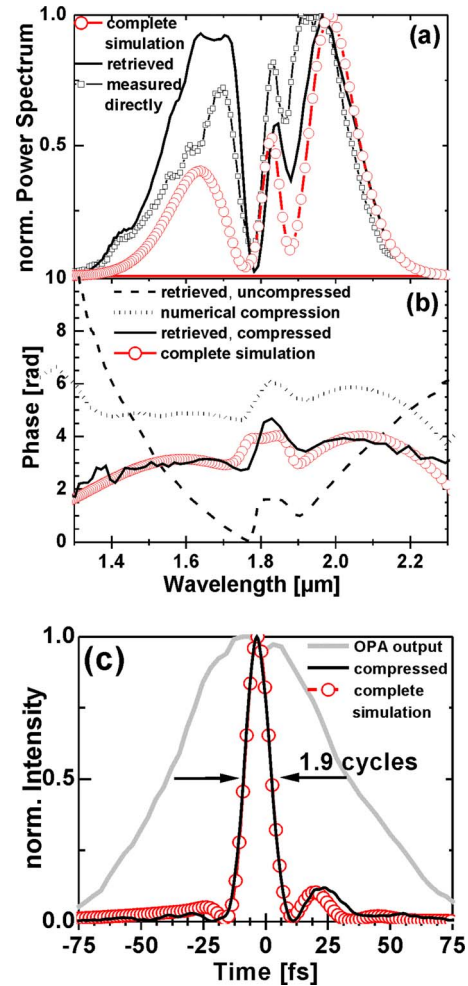


FIG. 3. (Color online) (a) Power spectral densities after nonlinear propagation in the HCF. (b) SHG-FROG retrieved spectral phases for uncompressed (black dashed line) and compressed pulses (black solid line) are compared with full numerical simulations (circles). The spectral phase named numerical compression (black dotted line) has been obtained by numerically propagating the retrieval of the uncompressed pulse (dashed line) through 3 mm of FS. (c) Temporal intensities corresponding to the spectra given above whereby compression down to 11.5 fs is achieved with 3 mm FS after the HCF.

solid line in Fig. 3(b)] is significantly flattened with respect to the uncompressed phase (black dashed line). In the case of pure SPM, one would expect symmetric broadening of the power spectrum around the fundamental accompanied by a symmetric phase function. However, the uncompensated phase [black dashed line] is slightly steeper on the red side compared with the blue side. This spectral asymmetry of the uncompensated pulse corresponds to a temporal asymmetry whereby the pulse exhibits a much steeper trailing edge than the leading one. Linear propagating this pulse through 3 mm of FS generates a very short 11.5 fs pulse [solid black line in Fig. 3(c)]. The fairly clean compressed pulse contains 78% of total energy in the main part and the FWHM duration is only 1.14 times the TL duration of 10.1 fs. Residual higher order phases which are not compensated by the bulk compressor are likely to cause the small pedestals on both sides of the main pulse. We mention that in addition to the rather clean temporal shape on the femtosecond time scale, the present approach is free of superfluorescence background as was reported in case of OPCPA.⁵ When the seed is blocked in the OPA, no light is observed at the output of the fiber.

It is pointed out that this almost TL and relatively clean temporal shape is remarkable because it denotes dispersion compensation not only of the GDD but also of the TOD to a large extent. Most of the commonly used glasses, like FS, exhibit normal dispersion ($GDD > 0$) below $1 \mu\text{m}$ and anomalous dispersion ($GDD < 0$) beyond the zero dispersion wavelength centered between $1.2\text{--}2 \mu\text{m}$. Thus bulk material is potentially suitable for pulse compression of IR laser pulses. However, all glasses exhibit positive TOD throughout their entire transmission range. Uncompensated TOD causes any femtosecond pulse to deviate from the TL pulse shape even if the GDD is zero. For instance, assuming a Gaussian shape at center wavelength of $1.83 \mu\text{m}$, a TOD of only 1000 fs^3 (3 mm FS plus 1 mm CaF_2) causes a TL pulse to broaden from 10.1 to 14.7 fs. To confirm that linear propagation through bulk material (intensity $\approx 5 \times 10^9 \text{ W/cm}^2$) compresses the pulse after the HCF, we calculated the spectral phase introduced by 3 mm of FS according to the Sellmeier equation. This phase was then added to the retrieved phase of the uncompressed pulse [black dashed curve in Fig. 3(b)]. The result [black dotted line in Fig. 3(b)] matches the retrieved phase of the compressed pulse. On the one hand, this numerical cross check proves the compression mechanism due to linear propagation in FS. On the other hand, it also demonstrates the reliability of the SHG-FROG retrieval though the retrieved power spectrum shows a lower peak on the blue side when compared to the directly measured spectrum. However, by comparing the retrieved spectral phase of compressed and uncompressed pulse we obtain the exact refractive index of FS in the range from 1.4 to $2.2 \mu\text{m}$. Now the question about the origin of the negative TOD component arises. To address this question, two possible explanations are discussed.

On the one hand, our experimental results might be viewed in the context of pulse self-compression. This explanation can be ruled out since we have to add 3 mm of FS subsequent to the HCF setup to obtain the shortest pulse. At $1.8 \mu\text{m}$, FS provides significant negative GDD ($-68 \text{ fs}^2/\text{mm}$). Furthermore, in contrast to experimentally observed self-compression,^{6,7,14,15} the laser power of 10 GW in our experiment is roughly two times below the estimated critical power for self-focusing.

On the other hand, the pronounced spectral asymmetry suggests that self-steepening^{15–17} of the pulse takes place in addition to SPM. This temporal reshaping of the trailing edge then leads to an asymmetric spectral phase opposed to the positive TOD of bulk material. To prove this qualitative explanation, we performed numerical simulations. The nonlinear Schrödinger equation¹⁸ was solved in one dimension where the action of self-steepening could be turned on and off numerically. Numerical results based on exact experimental conditions like input pulse duration, pulse energy, and pressure are given by the circles in Fig. 3 and a detailed description is in preparation for a longer article.¹⁹ Briefly, if self-steepening is neglected, it was not possible to simulate an asymmetric power spectrum as shown in Fig. 3(a). Contrary, the symmetry of the spectrum is broken because of self-steepening which is known to promote the higher frequency region of the spectrum.¹⁵ It furthermore enables calculating an asymmetric phase like the dashed curve of Fig. 3(b). Its linear propagation through 3 mm of FS leads to the plot shown by the circles in Fig. 3(b) which is in excellent

agreement with the experimentally retrieved phase [solid black line]. The corresponding temporal intensity [circles in Fig. 3(c)] closely resembles the experimentally retrieved pulse. Neglecting self-steepening leads to a pulse duration of 14.4 fs with an increased pedestal.

In conclusion, we have demonstrated a very simple and robust approach for the generation of submillijoule two-cycle $1.8 \mu\text{m}$ laser pulses via nonlinear propagation in a HCF followed by dispersion compensation utilizing the anomalous dispersion of bulk material. This straight forward approach was confirmed by numerical simulations that demonstrate the action of self-steepening is to generate a spectral phase opposite to that of FS. At the moment, our sub two-cycle laser pulses are not CEP stabilized, but this is feasible using the Idler of a white light seeded OPA.⁴

We are very grateful for the help and the time spent on the laser system by François Poitras and Antoine Laramée. The authors acknowledge the support of the Canada Foundation for Innovation, the Canadian Institute for Photonic Innovations, the Natural Sciences and Engineering Research Council of Canada, and the Fonds Québécois de la Recherche sur la Nature et les Technologies.

¹M. Hentschel, R. Kienberger, Ch. Spielmann, G. A. Reider, N. Milosevic, T. Brabec, P. B. Corkum, U. Heinzmann, M. Drescher, and F. Krausz, *Nature (London)* **414**, 509 (2001).

²G. Sansone, E. Benedetti, F. Calegari, C. Vozzi, L. Avaldi, R. Flammini, L. Poletto, P. Villoresi, C. Altucci, R. Vellota, S. Stagira, S. De Silvestri, and M. Nisoli, *Science* **314**, 443 (2006).

³E. Goulielmakis, M. Schultze, M. Hofstetter, V. S. Yakovlev, J. Gagnon, M. Uiberacker, A. L. Aquila, E. M. Gullikson, D. T. Attwood, R. Kienberger, F. Krausz, and U. Kleineberg, *Science* **320**, 1614 (2008).

⁴A. Baltuška, T. Fuji, and T. Kobayashi, *Phys. Rev. Lett.* **88**, 133901 (2002).

⁵X. Gu, G. Marcus, Y. Deng, T. Metzger, C. Teisset, N. Ishii, T. Fuji, A. Baltuška, R. Butkus, V. Pervak, H. Ishizuki, T. Taira, T. Kobayashi, R. Kienberger, and F. Krausz, *Opt. Express* **17**, 62 (2009).

⁶C. P. Hauri, R. B. Lopez-Martens, C. I. Blaga, K. D. Schultz, J. Cryan, R. Chirla, P. Colosimo, G. Doumy, A. M. March, C. Roedig, E. Sistrunk, J. Tate, J. Wheeler, L. F. Di Mauro, and E. P. Power, *Opt. Lett.* **32**, 868 (2007).

⁷O. D. Mücke, S. Ališauskas, A. J. Verhoef, A. Pugžlys, A. Baltuška, V. Smilgevičius, J. Pocius, L. Giniūnas, R. Danielius, and N. Forget, *Opt. Lett.* **34**, 2498 (2009).

⁸C. Vozzi, F. Calegari, E. Benedetti, S. Gasilov, G. Sansone, G. Cerullo, M. Nisoli, S. De Silvestri, and S. Stagira, *Opt. Lett.* **32**, 2957 (2007).

⁹M. Giguère, B. E. Schmidt, A. D. Shiner, M.-A. Houle, H.-C. Bandulet, G. Tempea, D. M. Villeneuve, J.-C. Kieffer, and F. Légaré, *Opt. Lett.* **34**, 1894 (2009).

¹⁰N. Demirdöven, M. Khalil, O. Golonzka, and A. Tokmakoff, *Opt. Lett.* **27**, 433 (2002).

¹¹R. Trebino, K. W. DeLong, D. N. Fittinghoff, J. N. Sweetser, M. A. Krumhügel, B. A. Richman, and D. J. Kane, *Rev. Sci. Instrum.* **68**, 3277 (1997).

¹²I. Z. Kozma, P. Baum, U. Schmidhammer, S. Lochbrunner, and E. Riedle, *Rev. Sci. Instrum.* **75**, 2323 (2004).

¹³A. Baltuška, M. S. Pshenichnikov, and D. A. Wiersma, *Opt. Lett.* **23**, 1474 (1998).

¹⁴N. L. Wagner, E. A. Gibson, T. Popmintchev, I. P. Christov, M. M. Murnane, and H. C. Kapteyn, *Phys. Rev. Lett.* **93**, 173902 (2004).

¹⁵G. Yang and Y. R. Shen, *Opt. Lett.* **9**, 510 (1984); G. Stibenz, N. Zhavoronkov, and G. Steinmeyer, *Opt. Lett.* **31**, 274 (2006).

¹⁶N. Aközbe, M. Scalora, C. M. Bowden, and S. L. Chin, *Opt. Commun.* **191**, 353 (2001).

¹⁷A. L. Gaeta, *Phys. Rev. Lett.* **84**, 3582 (2000).

¹⁸G. P. Agrawal, *Nonlinear Fiber Optics*, 3rd ed. (Academic, San Diego (2001)).

¹⁹P. Béjot, B. E. Schmidt, J. Kasparian, J.-P. Wolf, P. B. Corkum, and F. Légaré, "IR pulse compression with bulk material: Experiments versus simulations," (unpublished).